Copyright © 2006 Tech Science Press CMES, vol.12, no.3, pp.161-179, 2006

Computing Prager's Kinematic Hardening Mixed-Control Equations in a Pseudo-Riemann Manifold

Chein-Shan Liu[1]

Abstract: Materials' internal spacetime may bear certain similarities with the external spacetime of special relativity theory. Previously, it is shown that material hardening and anisotropy may cause the internal spacetime curved. In this paper we announce the third mechanism of mixed-control to cause the curvedness of internal spacetime. To tackle the mixed-control problem for a Prager kinematic hardening material, we demonstrate two new formulations. By using two-integrating factors idea we can derive two Lie type systems in the product space of $\mathbb{M}^{m+1}\otimes\mathbb{M}^{n+1}$. The Lie algebra is a direct sum of $so(m,1)\oplus so(n,1)$, and correspondingly the symmetry group is a direct product of $SO_o(m,1)\otimes SO_o(n,1)$, which left acts on a twin-cone. Then, by using the one-integrating factor idea we can convert the nonlinear constitutive equations into a Lie type system of $\dot{\mathbf{Z}}=\mathbf{CZ}$ with $\mathbf{C}\in sl(5,1,\mathbb{R})$ a Lie algebra of the special orthochronous pseudo-linear group $SL(5,1,\mathbb{R})$. The underlying space is a distorted cone in the pseudo-Riemann manifold. Consistent numerical methods are then developed according to these Lie symmetries, and numerical examples are used to assess the performance of new algorithms. The measures in terms of the errors by satisfying the consistency condition, strain and stress relative errors and orientational errors confirm that the new numerical methods are better than radial return method.

keyword: Prager kinematic hardening rule, Integrating factors, Mixed-controls, Pseudo-Riemann manifold, Internal spacetime, Internal symmetry, Consistent numerical schemes

1 Introduction

While a full stress control is not suitable for materials with strain softening, a full strain control is almost impossible to execute in real experimental testing of materials. Hence, by the strain control we usually refer to specifying just part of strain components and allowing to be zero of these stress components which are conjugate to the unspecified strain components. A mixed-control is a prescription of part of strain components and a simultaneous prescription of part of stress components conjugate to the unspecified strain components.

After introducing an elastoplastic model with Prager's kinematic hardening rule (Prager, 1956), our task is to find the response path as output from the constitutive relations when the stress-strain mixed-control path is prescribed as input. In the open literature, the subject of plasticity under mixed-controls has been investigated by Klisinski *et al.* (1992) and Klisinski (1998), and an integration algorithm under mixed-controls has been discussed by Ritto-Corrêa and Camotim (2001). It is important that in the experimental testing of materials a mixed-control is frequently used; for example, the uniaxial stress test is the simplest one of mixed-control. Upon recognizing this point we are naturally led to study the material behavior and response under mixed-controls.

In terms of five-dimensional stress and strain vectors, the material endowed with Prager's kinematic hardening rule can be modeled by [Hong and Liu (1999a); Liu (2005)]:

$$\dot{\mathbf{e}}=\dot{\mathbf{e}}^e+\dot{\mathbf{e}}^p, \tag{1}$$

$$\mathbf{s}=\boldsymbol{\xi}+\boldsymbol{\alpha}, \tag{2}$$

$$\dot{\mathbf{s}}=k_e\dot{\mathbf{e}}^e, \tag{3}$$

$$\boldsymbol{\xi}\dot{\lambda}=\xi_0\dot{\mathbf{e}}^p, \tag{4}$$

$$\dot{\boldsymbol{\alpha}}=k_b\dot{\mathbf{e}}^p, \tag{5}$$

$$\|\boldsymbol{\xi}\|\le\xi_0, \tag{6}$$

$$\dot{\lambda}\ge 0, \tag{7}$$

[1] Department of Mechanical and Mechatronic Engineering, Taiwan Ocean University, Keelung, Taiwan

$$\|\boldsymbol{\xi}\|\dot{\lambda} = \xi_0\dot{\lambda}. \tag{8}$$

There appear three material constants of k_e, k_b and ξ_0 in this material model.

The boldfaced $\mathbf{e}$, $\mathbf{e}^e$, $\mathbf{e}^p$, $\mathbf{s}$, $\boldsymbol{\xi}$ and $\boldsymbol{\alpha}$ are respectively the five-dimensional vectors of strains, elastic strains, plastic strains, stresses, active stresses and back stresses, whereas λ is a scalar called the equivalent plastic strain, with $\xi_0\dot{\lambda}$ being the specific power dissipation.

The concept of internal spacetime as advocated by Hong and Liu (1999a, 1999b, 2000) to model materials' plastic behaviors bears certain similarities with the external spacetime structure originated from the Einstein's landmark theory of special relativity (Hong and Liu, 2001). Both spacetimes are flat Minkowski spaces and the action groups are both of the Lorentz types, but with different dimensions.

Recent studies indicate that materials' internal spacetime due to isotropic hardening (Liu, 2003) or anisotropy (Liu, 2004c; Liu and Chang, 2005) cannot be flattened into a flat one. In addition, there is a third possibility to cause a curved internal spacetime due to an external stress-strain mixed-control imposing on materials. A common language to describe the curved spacetimes is a mathematical theory of pseudo-Riemann manifold. Essentially, the pseudo-Riemann manifold is a differentiable manifold equipped with a non-degenerate and non-positive metric tensor (Lang, 1999). Because the metric tensor is non-constant, the resulting spacetime is also non-flat. To demonstrate the third mechanism to cause the non-flatness of internal spacetime, the material elastoplastic model with Prager's kinematic hardening is a good choice, because this model allows stress-strain mixed-controls and the yield surface is always constant in the active stress space without considering isotropic hardening and anisotropy. Therefore, the latter two reasons to cause the non-flatness of internal spacetime just mentioned above can be ruled out, and we can concentrate our study on the third reason of mixed-control to cause the non-flatness of internal spacetime.

In this paper we analyze the above rate-form constitutive equations under strain-control in Section 2, stress-control in Section 3, and then stress-strain mixed-control in all subsequent sections. In Section 4 we derive a mixed stress-strain control equation. In Section 5 we propose a two integrating factors method to quasi-linearize the mixed stress-strain control equation, where the twin-cone structure and the symmetry group in a product space of $\mathbb{M}^{m+1}\otimes\mathbb{M}^{n+1}$ are discussed, and then a group-preserving scheme is derived. In Section 6 we use an integrating factor idea to form the constitutive equations under mixed-control in a pseudo-Riemann manifold, and then a consistent numerical scheme is developed. In Section 7 we derive a radial return method to integrate the constitutive equations under mixed-control. Section 8 demonstrates the performance of these numerical schemes by numerical examples. Finally, we draw conclusions in Section 9. This paper may provide us a deeper understanding of the underlying structure of an elastoplastic model with Prager's kinematic hardening under mixed-controls.

2 Exact linearization under strain control

2.1 *Expressed the responses in terms of* $\boldsymbol{\xi}$

From Eqs. (1)-(3) and (5) it follows that

$$\frac{1}{k_e}\dot{\mathbf{s}} + \frac{1}{k_b}(\dot{\mathbf{s}} - \dot{\boldsymbol{\xi}}) = \dot{\mathbf{e}}, \tag{9}$$

$$\frac{1}{k_e}(\dot{\boldsymbol{\xi}} + \dot{\boldsymbol{\alpha}}) + \frac{1}{k_b}\dot{\boldsymbol{\alpha}} = \dot{\mathbf{e}}, \tag{10}$$

$$\dot{\boldsymbol{\xi}} + k_b\dot{\mathbf{e}}^p = k_e(\dot{\mathbf{e}} - \dot{\mathbf{e}}^p). \tag{11}$$

Once $\boldsymbol{\xi}(t)$ can be obtained, it is easy to compute $\mathbf{s}(t)$, $\boldsymbol{\alpha}(t)$ and $\mathbf{e}^p(t)$ via the following formulae (Liu, 2002):

$$\mathbf{s}(t) = \mathbf{s}(t_i) + \beta[\boldsymbol{\xi}(t) - \boldsymbol{\xi}(t_i)] + \beta k_b[\mathbf{e}(t) - \mathbf{e}(t_i)], \tag{12}$$

$$\boldsymbol{\alpha}(t) = \boldsymbol{\alpha}(t_i) + (1-\beta)[\boldsymbol{\xi}(t_i) - \boldsymbol{\xi}(t)] + \beta k_b[\mathbf{e}(t) - \mathbf{e}(t_i)], \tag{13}$$

$$\mathbf{e}^p(t) = \mathbf{e}^p(t_i) + \frac{1}{k_e + k_b}[\boldsymbol{\xi}(t_i) - \boldsymbol{\xi}(t)] + \beta[\mathbf{e}(t) - \mathbf{e}(t_i)], \tag{14}$$

where $\beta = k_e/(k_e + k_b)$. They were obtained by integrating Eqs. (9)-(11). Here t is the current time and t_i is an initial time, at which the initial conditions of $\boldsymbol{\xi}(t_i)$, $\boldsymbol{\alpha}(t_i)$, $\mathbf{e}^p(t_i)$ and $\lambda(t_i)$ should be prescribed. The above three equations indicate that the responses are fully determined by $\boldsymbol{\xi}$ under strain control.

2.2 Linear system under strain control

Inserting the plastic flow rule (4) for $\dot{\mathbf{e}}^p$ into Eq. (11) we obtain

$$\dot{\boldsymbol{\xi}} + \frac{(k_e + k_b)\dot{\lambda}}{\xi_0}\boldsymbol{\xi} = k_e\dot{\mathbf{e}}. \tag{15}$$

The inner product of $\boldsymbol{\xi}$ with Eq. (15) is

$$\boldsymbol{\xi}\cdot\dot{\boldsymbol{\xi}} + \frac{(k_e + k_b)\dot{\lambda}}{\xi_0}\boldsymbol{\xi}\cdot\boldsymbol{\xi} = k_e\boldsymbol{\xi}\cdot\dot{\mathbf{e}}, \tag{16}$$

which, due to the constancy of ξ_0, asserts that

$$\dot{\lambda} = \frac{\beta}{\xi_0}\boldsymbol{\xi}\cdot\dot{\mathbf{e}} > 0 \text{ if } \|\boldsymbol{\xi}\| = \xi_0 \text{ and } \boldsymbol{\xi}\cdot\dot{\mathbf{e}} > 0, \tag{17}$$

$$\dot{\lambda} = 0 \text{ if } \|\boldsymbol{\xi}\| < \xi_0 \text{ or } \boldsymbol{\xi}\cdot\dot{\mathbf{e}} \le 0. \tag{18}$$

They are switching criteria of plastic irreversibility under strain control.

For Eq. (15) we can define an integrating factor:

$$Y := \exp\left(\frac{k_e + k_b}{\xi_0}\lambda\right), \tag{19}$$

such that it becomes

$$\frac{d}{dt}(Y\boldsymbol{\xi}) = k_e Y\dot{\mathbf{e}}. \tag{20}$$

On the other hand, Eq. (17) changes for Y into

$$\dot{Y} = \frac{k_e Y}{\xi_0^2}\boldsymbol{\xi}\cdot\dot{\mathbf{e}}. \tag{21}$$

Introduce

$$\mathbf{X} = \begin{bmatrix} \mathbf{X}^s \\ X^0 \end{bmatrix} = \begin{bmatrix} X^1 \\ \cdot \\ \cdot \\ \cdot \\ X^5 \\ X^0 \end{bmatrix} := \begin{bmatrix} Y\xi_1 \\ \cdot \\ \cdot \\ \cdot \\ Y\xi_5 \\ Y\xi_0 \end{bmatrix} \tag{22}$$

as the $5+1$-dimensional augmented state vector. Thus, from Eqs. (20) and (21) we have

$$\dot{\mathbf{X}} = \mathbf{A}\mathbf{X} \tag{23}$$

with

$$\mathbf{A} := \frac{k_e}{\xi_0}\begin{bmatrix} \mathbf{0}_5 & \dot{\mathbf{e}} \\ \dot{\mathbf{e}}^{\mathrm{T}} & 0 \end{bmatrix}. \tag{24}$$

Here, the superscript T denotes the transpose and $\mathbf{0}_5$ is a zero matrix with dimensions five. It can be seen that in this augmented space of $\mathbf{X} = (Y\boldsymbol{\xi}^{\mathrm{T}}, Y\xi_0)^{\mathrm{T}}$ the governing equations become linear and therefore tractable more easy than the original nonlinear equations.

The above procedure to exactly linearize the nonlinear constitutive equations in the space of $\mathbf{X}$ has been first developed by Hong and Liu (1999a).

3 Exact linearization under stress control

3.1 Expressed the responses in terms of $\boldsymbol{\xi}$

From Eqs. (2), (5) and (4) it follows that

$$\dot{\boldsymbol{\xi}} + \frac{k_b\dot{\lambda}}{\xi_0}\boldsymbol{\xi} = \dot{\mathbf{s}}, \tag{25}$$

or

$$\frac{d}{dt}(y\boldsymbol{\xi}) = y\dot{\mathbf{s}}, \tag{26}$$

in terms of another integrating factor:

$$y := \exp\left(\frac{k_b}{\xi_0}\lambda\right). \tag{27}$$

Once $\boldsymbol{\xi}(t)$ can be obtained, it is easy to directly compute

$$\boldsymbol{\alpha}(t) = \mathbf{s}(t) - \boldsymbol{\xi}(t), \tag{28}$$

$$\mathbf{e}(t) = \mathbf{e}(t_i) + \frac{1}{\beta k_b}[\mathbf{s}(t) - \mathbf{s}(t_i)] + \frac{1}{k_b}[\boldsymbol{\xi}(t_i) - \boldsymbol{\xi}(t)], \tag{29}$$

$$\mathbf{e}^p(t) = \mathbf{e}^p(t_i) + \frac{1}{k_b}[\mathbf{s}(t) - \mathbf{s}(t_i)] + \frac{1}{k_b}[\boldsymbol{\xi}(t_i) - \boldsymbol{\xi}(t)]. \tag{30}$$

The second equation is obtained from Eq. (12), and the third equation is obtained from Eqs. (14) and (29). Similarly, the above three equations indicate that the responses are fully determined by $\boldsymbol{\xi}$ under stress control.

3.2 Linear system under stress control

The inner product of $\boldsymbol{\xi}$ with Eq. (25) is

$$\boldsymbol{\xi}\cdot\dot{\boldsymbol{\xi}} + \frac{k_b\dot{\lambda}}{\xi_0}\boldsymbol{\xi}\cdot\boldsymbol{\xi} = \boldsymbol{\xi}\cdot\dot{\mathbf{s}}, \tag{31}$$

which, due to the constancy of ξ_0, asserts that

$$\dot{\lambda} = \frac{1}{k_b\xi_0}\boldsymbol{\xi}\cdot\dot{\mathbf{s}} > 0 \text{ if } \|\boldsymbol{\xi}\| = \xi_0 \text{ and } \boldsymbol{\xi}\cdot\dot{\mathbf{s}} > 0, \tag{32}$$

$$\dot{\lambda}=0 \text{ if } \|\boldsymbol{\xi}\|<\xi_0 \text{ or } \boldsymbol{\xi}\cdot\dot{\mathbf{s}}\le 0. \tag{33}$$

They are switching criteria of plastic irreversibility under stress control.

Eq. (32) can be expressed in terms of y defined by Eq. (27) as

$$\dot{y}=\frac{y}{\xi_0^2}\boldsymbol{\xi}\cdot\dot{\mathbf{s}}. \tag{34}$$

Let

$$\mathbf{x}=\begin{bmatrix}\mathbf{x}^s\\ x^0\end{bmatrix}=\begin{bmatrix}x^1\\ \cdot\\ \cdot\\ \cdot\\ x^5\\ x^0\end{bmatrix}:=\begin{bmatrix}y\xi_1\\ \cdot\\ \cdot\\ \cdot\\ y\xi_5\\ y\xi_0\end{bmatrix} \tag{35}$$

be another $5+1$-dimensional augmented state vector. Thus, from Eqs. (26) and (34) it follows that

$$\dot{\mathbf{x}}=\mathbf{B}\mathbf{x}, \tag{36}$$

where

$$\mathbf{B}:=\frac{1}{\xi_0}\begin{bmatrix}\mathbf{0}_5 & \dot{\mathbf{s}}\\ \dot{\mathbf{s}}^{\mathrm{T}} & 0\end{bmatrix}. \tag{37}$$

It can be seen that in this augmented space of $\mathbf{x}=(y\boldsymbol{\xi}^{\mathrm{T}},y\xi_0)^{\mathrm{T}}$ the governing equations are also linear.

4 Mixed stress-strain control equation

To properly address all kinds of controls we define the control path by

$$\mathbf{u}:=k_e\mathbf{P}^e\mathbf{e}+\mathbf{P}^s\mathbf{s}, \tag{38}$$

where $\mathbf{P}^e$ and $\mathbf{P}^s$ are the second-order tensors which are disjoint projection operators, namely,

$$\mathbf{P}^e\mathbf{P}^e=\mathbf{P}^e, \tag{39}$$

$$\mathbf{P}^s\mathbf{P}^s=\mathbf{P}^s, \tag{40}$$

$$\mathbf{P}^e+\mathbf{P}^s=\mathbf{I}_5, \tag{41}$$

$$\mathbf{P}^e\mathbf{P}^s=\mathbf{P}^s\mathbf{P}^e=\mathbf{0}_5. \tag{42}$$

$\mathbf{P}^e$ can be represented by a diagonal matrix with (Naylor and Sell, 1982)

$$\mathbf{P}^e=\begin{bmatrix}\lambda_1 & 0 & 0 & 0 & 0\\ 0 & \lambda_2 & 0 & 0 & 0\\ 0 & 0 & \lambda_3 & 0 & 0\\ 0 & 0 & 0 & \lambda_4 & 0\\ 0 & 0 & 0 & 0 & \lambda_5\end{bmatrix}, \tag{43}$$

where the elements $\lambda_i, i=1,\ldots,5$, are either 0 or 1. In the later the abbreviation of $\mathbf{P}^e=\text{diag}\,[\lambda_1,\lambda_2,\lambda_3,\lambda_4,\lambda_5]$ will be used.

Multiplying Eq. (15) by $\mathbf{P}^e$ we obtain

$$\mathbf{P}^e\dot{\boldsymbol{\xi}}+\frac{(k_e+k_b)\dot{\lambda}}{\xi_0}\mathbf{P}^e\boldsymbol{\xi}=k_e\mathbf{P}^e\dot{\mathbf{e}}. \tag{44}$$

Similarly, multiplying Eq. (25) by $\mathbf{P}^s$ we obtain

$$\mathbf{P}^s\dot{\boldsymbol{\xi}}+\frac{k_b\dot{\lambda}}{\xi_0}\mathbf{P}^s\boldsymbol{\xi}=\mathbf{P}^s\dot{\mathbf{s}}. \tag{45}$$

Then, the sum of these two resultants yields

$$\dot{\boldsymbol{\xi}}+\frac{(k_e+k_b)\dot{\lambda}}{\xi_0}\mathbf{P}^e\boldsymbol{\xi}+\frac{k_b\dot{\lambda}}{\xi_0}\mathbf{P}^s\boldsymbol{\xi}=\dot{\mathbf{u}}. \tag{46}$$

Substituting $\mathbf{P}^s=\mathbf{I}_5-\mathbf{P}^e$ into the left-hand side of the above equation, and inserting it for $\dot{\boldsymbol{\xi}}$ into the consistency condition $\boldsymbol{\xi}\cdot\dot{\boldsymbol{\xi}}=0$, leads to

$$H_m\dot{\lambda}=\boldsymbol{\xi}\cdot\dot{\mathbf{u}}, \tag{47}$$

where

$$H_m:=\frac{k_e}{\xi_0}\boldsymbol{\xi}\cdot\mathbf{P}^e\boldsymbol{\xi}+k_b\xi_0 \tag{48}$$

is the stability function for stress-strain mixed-control equation.

Supposing $H_m>0$, from Eq. (47) we can deduce the following on-off switching criteria of plastic irreversibility:

$$\dot{\lambda}=\frac{\boldsymbol{\xi}\cdot\dot{\mathbf{u}}}{H_m}>0 \text{ if } \|\boldsymbol{\xi}\|=\xi_0 \text{ and } \boldsymbol{\xi}\cdot\dot{\mathbf{u}}>0, \tag{49}$$

$$\dot{\lambda}=0 \text{ if } \|\boldsymbol{\xi}\|<\xi_0 \text{ or } \boldsymbol{\xi}\cdot\dot{\mathbf{u}}\le 0. \tag{50}$$

In the on phase of the switch, $\dot{\lambda}>0$, the mechanism of plastic irreversibility is working and the material exhibits an elastoplastic behavior, while in the off phase of

the switch, $\dot{\lambda}=0$, the material deformation is reversible and elastic. According to the complementary trio (6)-(8), there are just two phases: (i) $\dot{\lambda}>0$ and $\|\boldsymbol{\xi}\|=\xi_0$, and (ii) $\dot{\lambda}=0$ and $\|\boldsymbol{\xi}\|\le\xi_0$. From criteria (49) and (50) it is clear that (i) corresponds to the on phase whereas (ii) to the off phase.

The mixed-control problem is for a given $\mathbf{P}^e\mathbf{e}(t)$ and $\mathbf{P}^s\mathbf{s}(t)$ to find $\mathbf{P}^e\mathbf{s}(t)$ and $\mathbf{P}^s\mathbf{e}(t)$, which can be obtained by multiplying Eq. (12) by $\mathbf{P}^e$ and Eq. (29) by $\mathbf{P}^s$:

$$\begin{aligned}\mathbf{P}^e\mathbf{s}(t)&=\mathbf{P}^e\mathbf{s}(t_i)+\beta[\mathbf{P}^e\boldsymbol{\xi}(t)-\mathbf{P}^e\boldsymbol{\xi}(t_i)]\\&\quad+\beta k_b[\mathbf{P}^e\mathbf{e}(t)-\mathbf{P}^e\mathbf{e}(t_i)],\end{aligned}\tag{51}$$

$$\begin{aligned}\mathbf{P}^s\mathbf{e}(t)&=\mathbf{P}^s\mathbf{e}(t_i)+\frac{1}{\beta k_b}[\mathbf{P}^s\mathbf{s}(t)-\mathbf{P}^s\mathbf{s}(t_i)]\\&\quad+\frac{1}{k_b}[\mathbf{P}^s\boldsymbol{\xi}(t_i)-\mathbf{P}^s\boldsymbol{\xi}(t)].\end{aligned}\tag{52}$$

The back stress can be obtained by multiplying Eq. (13) by $\mathbf{P}^e$, multiplying $\boldsymbol{\alpha}(t)=\mathbf{s}(t)-\boldsymbol{\xi}(t)$ by $\mathbf{P}^s$, and adding these two resultants together as

$$\begin{aligned}\boldsymbol{\alpha}(t)&=\mathbf{P}^e\boldsymbol{\alpha}(t_i)+\mathbf{P}^s\mathbf{s}(t)-\mathbf{P}^s\boldsymbol{\xi}(t)\\&\quad+(1-\beta)[\mathbf{P}^e\boldsymbol{\xi}(t_i)-\mathbf{P}^e\boldsymbol{\xi}(t)]\\&\quad+\beta k_b[\mathbf{P}^e\mathbf{e}(t)-\mathbf{P}^e\mathbf{e}(t_i)].\end{aligned}\tag{53}$$

Similarly, the plastic strain can be obtained by multiplying Eq. (14) by $\mathbf{P}^e$, multiplying Eq. (30) by $\mathbf{P}^s$, and adding these two resultants together as

$$\begin{aligned}\mathbf{e}^p(t)&=\mathbf{e}^p(t_i)+\frac{1}{k_e+k_b}[\mathbf{P}^e\boldsymbol{\xi}(t_i)-\mathbf{P}^e\boldsymbol{\xi}(t)]\\&\quad+\beta[\mathbf{P}^e\mathbf{e}(t)-\mathbf{P}^e\mathbf{e}(t_i)]+\frac{1}{k_b}[\mathbf{P}^s\mathbf{s}(t)-\mathbf{P}^s\mathbf{s}(t_i)]\\&\quad+\frac{1}{k_b}[\mathbf{P}^s\boldsymbol{\xi}(t_i)-\mathbf{P}^s\boldsymbol{\xi}(t)].\end{aligned}\tag{54}$$

Thus, upon substituting $\boldsymbol{\xi}$, $\mathbf{P}^e\mathbf{e}$ and $\mathbf{P}^s\mathbf{s}$ into Eqs. (51)-(54) we obtain $\mathbf{P}^e\mathbf{s}$, $\mathbf{P}^s\mathbf{e}$, $\boldsymbol{\alpha}$ and $\mathbf{e}^p$.

It can be seen that the problem of finding responses under mixed-controls is still fully determined by $\mathbf{P}^e\boldsymbol{\xi}$ and $\mathbf{P}^s\boldsymbol{\xi}$ under the inputs of $\mathbf{P}^e\dot{\mathbf{e}}$ and $\mathbf{P}^s\dot{\mathbf{s}}$ as shown in Fig. 1. However, this problem becomes difficult because Eqs. (44) and (45) exhibit two different moduli of k_e+k_b and k_b, which corresponding to mixed strain and stress controls.

When inserting Eq. (49) for $\dot{\lambda}$ into Eq. (46) we obtain

$$\dot{\boldsymbol{\xi}}+\frac{(k_e+k_b)\boldsymbol{\xi}\cdot\dot{\mathbf{u}}}{\xi_0 H_m}\mathbf{P}^e\boldsymbol{\xi}+\frac{k_b\boldsymbol{\xi}\cdot\dot{\mathbf{u}}}{\xi_0 H_m}\mathbf{P}^s\boldsymbol{\xi}=\dot{\mathbf{u}}.\tag{55}$$

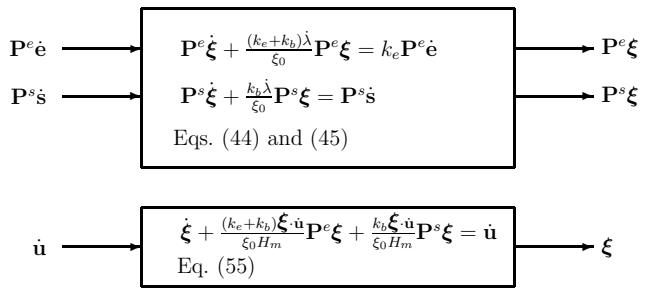

Figure 1 : Schematic drawings to show the block diagrams of a mixed-control problem.

The problem is that for the specified mixed-control input of $\dot{\mathbf{u}}$ we must solve $\boldsymbol{\xi}$ as shown in Fig. 1.

Both $H_m=(k_e+k_b)\xi_0$ for strain control and $H_m=k_b\xi_0$ for stress control are constant, and the above equation can be linearized as shown in Section 2 for strain-control and Section 3 for stress-control. However, for mixed-controls H_m is a function of $\boldsymbol{\xi}$, which renders the above equation highly nonlinear. If one does not use a specifically designed numerical method to integrate the above constitutive equation, then the yield condition of $\|\boldsymbol{\xi}\|=\xi_0$ may not be guaranteed for all time in the plastic phase.

5 Two integrating factors formulation

Unlike the strain or stress control case, each of which can be exactly linearized in an augmented active stress space as shown in Eqs. (23) and (36), respectively, the governing equation (46) for the mixed-control case cannot be linearized exactly. The main obstacle lies in the fact that there are two different integrating factors of Y and y as defined, respectively, by Eqs. (19) and (27) appearing in Eq. (46) with the forms of $\dot{Y}/Y=(k_e+k_b)\dot{\lambda}/\xi_0$ and $\dot{y}/y=k_b\dot{\lambda}/\xi_0$, such that one of the procedures to linearize Eq. (15) to Eq. (20) or Eq. (25) to Eq. (26) is no more applicable for this mixed-control case. Physically speaking, the two augmented active stress spaces are endowed with different moduli: one with k_e+k_b and another one with k_b. However, we develop below two novel methods to quasi-linearize the governing equations for $\boldsymbol{\xi}$.

5.1 Quasi-linear mixed-control equation

First, the yield condition can be written as

$$\boldsymbol{\xi}\cdot\mathbf{P}^e\boldsymbol{\xi}+\boldsymbol{\xi}\cdot\mathbf{P}^s\boldsymbol{\xi}=\xi_0^2,\tag{56}$$

because of $\mathbf{P}^e + \mathbf{P}^s = \mathbf{I}_5$. Let

$$\xi_e^2 := \boldsymbol{\xi} \cdot \mathbf{P}^e \boldsymbol{\xi}, \tag{57}$$

$$\xi_s^2 := \boldsymbol{\xi} \cdot \mathbf{P}^s \boldsymbol{\xi}, \tag{58}$$

such that

$$\xi_e^2 + \xi_s^2 = \xi_0^2 \tag{59}$$

due to Eq. (56).

Multiplying Eq. (20) by $\mathbf{P}^e$ we obtain

$$\frac{d}{dt}(Y\mathbf{P}^e\boldsymbol{\xi}) = k_e Y \mathbf{P}^e \dot{\mathbf{e}}. \tag{60}$$

On the other hand, taking the inner product of Eq. (60) with $\mathbf{P}^e\boldsymbol{\xi}$, and noting that

$$\mathbf{P}^e\boldsymbol{\xi} \cdot \mathbf{P}^e\boldsymbol{\xi} = \xi_e^2,$$

$$\mathbf{P}^e\boldsymbol{\xi} \cdot \mathbf{P}^e\dot{\boldsymbol{\xi}} = \xi_e \dot{\xi}_e$$

due to Eq. (57) and $(\mathbf{P}^e)^2 = \mathbf{P}^e = (\mathbf{P}^e)^{\mathrm{T}}$, we obtain

$$\frac{d}{dt}(Y\xi_e) = \frac{k_e}{\xi_e} Y \mathbf{P}^e \dot{\mathbf{e}} \cdot \mathbf{P}^e \boldsymbol{\xi}. \tag{61}$$

Eqs. (60) and (61) can be combined together to a quasi-linear differential equations system:

$$\dot{\mathbf{X}}_e = \mathbf{A}_e \mathbf{X}_e \tag{62}$$

with

$$\mathbf{X}_e = \begin{bmatrix} \mathbf{X}_e^s \\ X_e^0 \end{bmatrix} := \begin{bmatrix} Y\mathbf{P}^e\boldsymbol{\xi} \\ Y\xi_e \end{bmatrix}, \tag{63}$$

$$\mathbf{A}_e := \frac{k_e}{\xi_e} \begin{bmatrix} \mathbf{0}_m & \mathbf{P}^e\dot{\mathbf{e}} \\ (\mathbf{P}^e\dot{\mathbf{e}})^{\mathrm{T}} & 0 \end{bmatrix}, \tag{64}$$

where m is the dimensions of strain-controlled space. Since $\mathbf{A}_e$ is slightly dependent on ξ_e, which is not a constant but an unknown function, Eq. (62), unlike the linear systems (23) and (36), is a quasi-linear system.

Similarly, multiplying Eq. (26) by $\mathbf{P}^s$ we obtain

$$\frac{d}{dt}(y\mathbf{P}^s\boldsymbol{\xi}) = y\mathbf{P}^s\dot{\mathbf{s}}. \tag{65}$$

Then, taking the inner product of Eq. (65) with $\mathbf{P}^s\boldsymbol{\xi}$, and noting that

$$\mathbf{P}^s\boldsymbol{\xi} \cdot \mathbf{P}^s\boldsymbol{\xi} = \xi_s^2,$$

$$\mathbf{P}^s\boldsymbol{\xi} \cdot \mathbf{P}^s\dot{\boldsymbol{\xi}} = \xi_s \dot{\xi}_s$$

due to Eq. (58) and $(\mathbf{P}^s)^2 = \mathbf{P}^s = (\mathbf{P}^s)^{\mathrm{T}}$, we obtain

$$\frac{d}{dt}(y\xi_s) = \frac{1}{\xi_s} y \mathbf{P}^s\dot{\mathbf{s}} \cdot \mathbf{P}^s\boldsymbol{\xi}. \tag{66}$$

Eqs. (65) and (66) can be combined together to a quasi-linear differential equations system:

$$\dot{\mathbf{X}}_s = \mathbf{A}_s \mathbf{X}_s \tag{67}$$

with

$$\mathbf{X}_s = \begin{bmatrix} \mathbf{X}_s^s \\ X_s^0 \end{bmatrix} := \begin{bmatrix} y\mathbf{P}^s\boldsymbol{\xi} \\ y\xi_s \end{bmatrix}, \tag{68}$$

$$\mathbf{A}_s := \frac{1}{\xi_s} \begin{bmatrix} \mathbf{0}_n & \mathbf{P}^s\dot{\mathbf{s}} \\ (\mathbf{P}^s\dot{\mathbf{s}})^{\mathrm{T}} & 0 \end{bmatrix}, \tag{69}$$

where n is the dimensions of stress-controlled space with $n = 5 - m$.

5.2 Twin-cone and symmetry groups

Both strain and stress control cases exhibit a cone structure in the augmented spaces of $\mathbf{X}$ and $\mathbf{x}$, respectively. From Eq. (22) we have

$$\mathbf{X}^{\mathrm{T}}\mathbf{g}\mathbf{X} = \|\mathbf{X}^s\|^2 - (X^0)^2 = Y^2[\|\boldsymbol{\xi}\|^2 - \xi_0^2], \tag{70}$$

where

$$\mathbf{g} = \begin{bmatrix} \mathbf{I}_5 & \mathbf{0}_{5\times 1} \\ \mathbf{0}_{1\times 5} & -1 \end{bmatrix} \tag{71}$$

is a six-dimensional indefinite metric tensor. The $5+1$-dimensional vector space of augmented active stress $\mathbf{X}$ endowed with the Minkowski metric $\mathbf{g}$ is referred to as Minkowski spacetime denoted by $\mathbb{M}^{5+1}$.

Regarding Eqs. (70) and (6), we may distinguish two correspondences:

$$\|\boldsymbol{\xi}\| = \xi_0 \iff \mathbf{X}^{\mathrm{T}}\mathbf{g}\mathbf{X} = 0, \tag{72}$$

$$\|\boldsymbol{\xi}\| < \xi_0 \iff \mathbf{X}^{\mathrm{T}}\mathbf{g}\mathbf{X} < 0. \tag{73}$$

That is, an active stress $\boldsymbol{\xi}$ on the yield hypersphere of $\|\boldsymbol{\xi}\| = \xi_0$ corresponds to an augmented active stress $\mathbf{X}$ on the right circular cone $\{\mathbf{X}|\ \mathbf{X}^{\mathrm{T}}\mathbf{g}\mathbf{X} = 0\}$ in the Minkowski space, whereas a $\boldsymbol{\xi}$ within the yield hypersphere corresponds to an $\mathbf{X}$ in the interior $\{\mathbf{X}|\ \mathbf{X}^{\mathrm{T}}\mathbf{g}\mathbf{X} < 0\}$ of the cone. The exterior $\{\mathbf{X}|\ \mathbf{X}^{\mathrm{T}}\mathbf{g}\mathbf{X} > 0\}$ of the cone is uninhabitable since $\|\boldsymbol{\xi}\| > \xi_0$ is forbidden according to Eq. (6).

Since $\mathbf{A}$ in Eq. (23) satisfying

$$\mathbf{A}^{\mathrm{T}}\mathbf{g} + \mathbf{g}\mathbf{A} = \mathbf{0} \tag{74}$$

is a six-dimensional Lie algebra of the proper orthochronous Lorentz group $SO_o(5,1)$, the $\mathbf{G}$ being the fundamental solution of Eq. (23) satisfies the following group properties (Liu, 2001):

$$\mathbf{G}^{\mathrm{T}}\mathbf{g}\mathbf{G} = \mathbf{g},\ \det\mathbf{G} = 1,\ G_0^0 \geq 1, \tag{75}$$

where det is the shorthand of determinant and G_0^0 is the 00th component of $\mathbf{G}$. A more detailed discussion about the internal symmetry groups of material models can be found in Hong and Liu (1999a, 1999b, 2000), Liu (2003, 2004a-d, 2005), Liu and Chang (2004, 2005) and Liu and Li (2005).

Similar results hold for stress control case. Now, we turn our attention to the mixed-control case. From Eqs. (63) and (68) it follows that

$$\mathbf{X}_e^{\mathrm{T}}\mathbf{g}_e\mathbf{X}_e = \|\mathbf{X}_e^s\|^2 - (X_e^0)^2 = Y^2[\|\mathbf{P}^e\boldsymbol{\xi}\|^2 - \xi_e^2], \tag{76}$$

$$\mathbf{X}_s^{\mathrm{T}}\mathbf{g}_s\mathbf{X}_s = \|\mathbf{X}_s^s\|^2 - (X_s^0)^2 = y^2[\|\mathbf{P}^s\boldsymbol{\xi}\|^2 - \xi_s^2], \tag{77}$$

where

$$\mathbf{g}_e = \begin{bmatrix} \mathbf{I}_m & \mathbf{0}_{m\times 1} \\ \mathbf{0}_{1\times m} & -1 \end{bmatrix},\ \mathbf{g}_s = \begin{bmatrix} \mathbf{I}_n & \mathbf{0}_{n\times 1} \\ \mathbf{0}_{1\times n} & -1 \end{bmatrix} \tag{78}$$

are the $m+1$- and $n+1$-dimensional Minkowski metrics in the Minkowski spacetimes of $\mathbb{M}^{m+1}$ and $\mathbb{M}^{n+1}$, respectively.

By Eqs. (76), (77), (57) and (58) we may further distinguish two correspondences:

$$\|\mathbf{P}^e\boldsymbol{\xi}\| = \xi_e \iff \mathbf{X}_e^{\mathrm{T}}\mathbf{g}_e\mathbf{X}_e = 0, \tag{79}$$

$$\|\mathbf{P}^s\boldsymbol{\xi}\| = \xi_s \iff \mathbf{X}_s^{\mathrm{T}}\mathbf{g}_s\mathbf{X}_s = 0. \tag{80}$$

The former corresponds to a cone in the augmented space $\mathbf{X}_e$ of $\mathbb{M}^{m+1}$, while the latter a cone in the augmented space $\mathbf{X}_s$ of $\mathbb{M}^{n+1}$. Totally, in the augmented active stress space they composed as a *twin-cone*. When $\mathbf{P}^s = \mathbf{0}$, *i.e.*, strain control case, the twin-cone is collapsed into a single cone for $\mathbf{X}$, and conversely, when $\mathbf{P}^e = \mathbf{0}$, *i.e.*, stress control case, the twin-cone is collapsed into a single cone for $\mathbf{x}$. Conversely, we may also say that when a mixed-control problem is concerned with, the single cone in the space of $\mathbb{M}^{5+1}$ either for strain or stress control is split into a twin-cone in the space of $\mathbb{M}^{m+1} \otimes \mathbb{M}^{n+1}$, where $m+n = 5$.

Now, since $\mathbf{A}_e$ in Eq. (62) satisfying

$$\mathbf{A}_e^{\mathrm{T}}\mathbf{g}_e + \mathbf{g}_e\mathbf{A}_e = \mathbf{0} \tag{81}$$

is an $m+1$-dimensional Lie algebra of the proper orthochronous Lorentz group $SO_o(m,1)$, the $\mathbf{G}_e$ generated from Eq. (62) satisfies the following group properties:

$$\mathbf{G}_e^{\mathrm{T}}\mathbf{g}_e\mathbf{G}_e = \mathbf{g}_e,\ \det\mathbf{G}_e = 1,\ (G_e)_0^0 \geq 1. \tag{82}$$

Correspondingly, since $\mathbf{A}_s$ in Eq. (67) satisfying

$$\mathbf{A}_s^{\mathrm{T}}\mathbf{g}_s + \mathbf{g}_s\mathbf{A}_s = \mathbf{0} \tag{83}$$

is an $n+1$-dimensional Lie algebra of the proper orthochronous Lorentz group $SO_o(n,1)$, the $\mathbf{G}_s$ generated from Eq. (67) satisfies the following group properties:

$$\mathbf{G}_s^{\mathrm{T}}\mathbf{g}_s\mathbf{G}_s = \mathbf{g}_s,\ \det\mathbf{G}_s = 1,\ (G_s)_0^0 \geq 1. \tag{84}$$

In summary, we have used the two integrating factors method to derive two Lie type systems in the product space of $\mathbb{M}^{m+1} \otimes \mathbb{M}^{n+1}$. The Lie algebra is a direct sum of $so(m,1) \oplus so(n,1)$, and correspondingly the symmetry group is a direct product of $SO_o(m,1) \otimes SO_o(n,1)$, left acting on a twin-cone.

5.3 Group-preserving scheme

For the calculation purpose we may approximate the specified mixed-controlled path by a rectilinear path, such that $\mathbf{P}^e\dot{\mathbf{e}}$ and $\mathbf{P}^s\dot{\mathbf{s}}$ at each time increment are constant vectors, denoting by $\mathbf{P}^e\dot{\mathbf{e}}(\ell)$ and $\mathbf{P}^s\dot{\mathbf{s}}(\ell)$ at a discrete time $t = t_\ell$. The numerical scheme attempts to provide a medium to calculate the values of $\mathbf{X}_e$ and $\mathbf{X}_s$ at the next time $t = t_{\ell+1}$ when knowing $\mathbf{X}_e$ and $\mathbf{X}_s$ at time $t = t_\ell$.

The evolution of $\mathbf{X}_e$ is governed by Eq. (62) with matrix $\mathbf{A}_e$ given by Eq. (64). Due to the piecewise linearity

of controlled strain, $\mathbf{P}^e\dot{\mathbf{e}}$ is constant in each time increment equal to Δt. Unluckily, due to the presence of ξ_e in Eq. (64), this is not true for matrix $\mathbf{A}_e$. Therefore we approximate the solution of Eq. (62) by considering ξ_e as a constant in each single time step. Under such an additional hypothesis, the matrix $\mathbf{A}_e$ is constant, and so the evolution of Eq. (62) is known to be

$$\mathbf{X}_e(\ell+1) = \mathbf{G}_e(\ell)\mathbf{X}_e(\ell), \tag{85}$$

where

$$\begin{aligned}\mathbf{G}_e(\ell) &:= \exp[\Delta t\mathbf{A}_e(\ell)] \\ &= \begin{bmatrix} \mathbf{I}_m + \frac{[a_e(\ell)-1]}{\|\mathbf{P}^e\dot{\mathbf{e}}(\ell)\|^2}\mathbf{P}^e\dot{\mathbf{e}}(\ell)(\mathbf{P}^e\dot{\mathbf{e}}(\ell))^{\mathrm{T}} & \frac{b_e(\ell)\mathbf{P}^e\dot{\mathbf{e}}(\ell)}{\|\mathbf{P}^e\dot{\mathbf{e}}(\ell)\|} \\ \frac{b_e(\ell)(\mathbf{P}^e\dot{\mathbf{e}}(\ell))^{\mathrm{T}}}{\|\mathbf{P}^e\dot{\mathbf{e}}(\ell)\|} & a_e(\ell) \end{bmatrix},\end{aligned} \tag{86}$$

in which

$$a_e(\ell) := \cosh\left(\frac{k_e\Delta t\|\mathbf{P}^e\dot{\mathbf{e}}(\ell)\|}{\xi_e(\ell)}\right), \tag{87}$$

$$b_e(\ell) := \sinh\left(\frac{k_e\Delta t\|\mathbf{P}^e\dot{\mathbf{e}}(\ell)\|}{\xi_e(\ell)}\right). \tag{88}$$

A similar argument is applied to Eq. (67) with matrix $\mathbf{A}_s$ given by Eq. (69), leading to

$$\mathbf{X}_s(\ell+1) = \mathbf{G}_s(\ell)\mathbf{X}_s(\ell), \tag{89}$$

where

$$\begin{aligned}\mathbf{G}_s(\ell) &:= \exp[\Delta t\mathbf{A}_s(\ell)] \\ &= \begin{bmatrix} \mathbf{I}_n + \frac{[a_s(\ell)-1]}{\|\mathbf{P}^s\dot{\mathbf{s}}(\ell)\|^2}\mathbf{P}^s\dot{\mathbf{s}}(\ell)(\mathbf{P}^s\dot{\mathbf{s}}(\ell))^{\mathrm{T}} & \frac{b_s(\ell)\mathbf{P}^s\dot{\mathbf{s}}(\ell)}{\|\mathbf{P}^s\dot{\mathbf{s}}(\ell)\|} \\ \frac{b_s(\ell)(\mathbf{P}^s\dot{\mathbf{s}}(\ell))^{\mathrm{T}}}{\|\mathbf{P}^s\dot{\mathbf{s}}(\ell)\|} & a_s(\ell) \end{bmatrix},\end{aligned} \tag{90}$$

in which

$$a_s(\ell) := \cosh\left(\frac{\Delta t\|\mathbf{P}^s\dot{\mathbf{s}}(\ell)\|}{\xi_s(\ell)}\right), \tag{91}$$

$$b_s(\ell) := \sinh\left(\frac{\Delta t\|\mathbf{P}^s\dot{\mathbf{s}}(\ell)\|}{\xi_s(\ell)}\right). \tag{92}$$

However, in their current forms, Eqs. (85) and (89) are insufficient to determine the values of $\mathbf{P}^e\boldsymbol{\xi}(\ell+1)$ and $\mathbf{P}^s\boldsymbol{\xi}(\ell+1)$, since from Eqs. (63) and (68) we have

$$\mathbf{P}^e\boldsymbol{\xi}(\ell+1) = \frac{\mathbf{X}_e^s(\ell+1)}{X_e^0(\ell+1)}\xi_e(\ell+1), \tag{93}$$

$$\mathbf{P}^s\boldsymbol{\xi}(\ell+1) = \frac{\mathbf{X}_s^s(\ell+1)}{X_s^0(\ell+1)}\xi_s(\ell+1), \tag{94}$$

and there are still two unknowns of $\xi_e(\ell+1)$ and $\xi_s(\ell+1)$ on the right-hand sides. In order to solve this problem we need four equations:

$$Y(\ell+1)\xi_e(\ell+1) = X_e^0(\ell+1), \tag{95}$$

$$y(\ell+1)\xi_s(\ell+1) = X_s^0(\ell+1), \tag{96}$$

$$\xi_e^2(\ell+1) + \xi_s^2(\ell+1) = \xi_0^2, \tag{97}$$

$$y(\ell+1) - Y^{(1-\beta)}(\ell+1) = 0 \tag{98}$$

to solve the four unknowns of $\xi_e(\ell+1)$, $\xi_s(\ell+1)$, $Y(\ell+1)$ and $y(\ell+1)$. In above the values on right-hand sides are all known. Eq. (95) is obtained from the last one row in Eq. (63); Eq. (96) is obtained from the last one row in Eq. (68); Eq. (97) is a direct result of Eq. (59); and Eq. (98) is obtained by comparing Eq. (19) with Eq. (27). Substituting Eq. (96) for $\xi_s(\ell+1)$ into Eq. (97), where $y(\ell+1)$ is replaced by $Y^{(1-\beta)}(\ell+1)$ which is further replaced by $X_e^0(\ell+1)/\xi_e(\ell+1)$ due to Eq. (95), we obtain

$$\begin{aligned}F(\xi_e(\ell+1)) &:= \xi_e^2(\ell+1) \\ &+ \frac{(X_s^0(\ell+1))^2}{(X_e^0(\ell+1))^{2(1-\beta)}}\xi_e^{2(1-\beta)}(\ell+1) - \xi_0^2 = 0.\end{aligned} \tag{99}$$

Because of $F(0) = -\xi_0^2 < 0$ and $F(\xi_0) = (X_s^0(\ell+1))^2\xi_0^{2(1-\beta)}/(X_e^0(\ell+1))^{2(1-\beta)} > 0$, there must exist a real root of the above equation in the range of $0 < \xi_e(\ell+1) < \xi_0$.

Numerically solving Eq. (99) we obtain $\xi_e(\ell+1)$ and then $\xi_s(\ell+1)$ can be obtained from Eq. (97). Therefore, from Eq. (95) we obtain $Y(\ell+1)$, and from Eq. (96) we obtain $y(\ell+1)$. Substituting these two values of $\xi_e(\ell+1)$ and $\xi_s(\ell+1)$ into Eqs. (93) and (94) we can obtain $\mathbf{P}^e\boldsymbol{\xi}(\ell+1)$ and $\mathbf{P}^s\boldsymbol{\xi}(\ell+1)$, and hence $\boldsymbol{\xi}(\ell+1)$. Thus, substituting $\boldsymbol{\xi}$, $\mathbf{P}^e\mathbf{e}$ and $\mathbf{P}^s\mathbf{s}$ into Eqs. (51)-(54) we obtain $\mathbf{P}^e\mathbf{s}$, $\mathbf{P}^s\mathbf{e}$, $\boldsymbol{\alpha}$ and $\mathbf{e}^p$.

6 A pseudo-Riemann method

In Section 5 we have furnished a two-integrating-factor and a twin-cone formulation for mixed-control equations, and then derived a numerical scheme to implement it. In this section we attempt to unify the mixed-control equations from an integrating factor method and a single-cone formulation.

6.1 A pseudo-Riemann manifold

Multiplying Eqs. (20) and (26) by $\mathbf{P}^e$ and $\mathbf{P}^s$, respectively, and then letting

$$\mathbf{Z}^{s(m)} := Y\mathbf{P}^e\boldsymbol{\xi}, \tag{100}$$

$$\mathbf{Z}^{s(n)} := y\mathbf{P}^s\boldsymbol{\xi}, \tag{101}$$

where m and n indicate the dimensions of strain and stress control variables, we can obtain

$$\dot{\mathbf{Z}}^{s(m)} = k_e Y\mathbf{P}^e\dot{\mathbf{e}}, \tag{102}$$

$$\dot{\mathbf{Z}}^{s(n)} = y\mathbf{P}^s\dot{\mathbf{s}}. \tag{103}$$

The above y defined by Eq. (27) can be written as $y = Y^{(1-\beta)}$. Then, from Eqs. (19) and (47) it follows that

$$\frac{d}{dt}(Y\xi_0) = \frac{(k_e+k_b)Y}{H_m}\boldsymbol{\xi}\cdot\dot{\mathbf{u}}. \tag{104}$$

Upon introducing

$$\mathbf{Z} = \begin{bmatrix} \mathbf{Z}^{s(m)} \\ \mathbf{Z}^{s(n)} \\ Z^0 \end{bmatrix} = \begin{bmatrix} Y\mathbf{P}^e\boldsymbol{\xi} \\ y\mathbf{P}^s\boldsymbol{\xi} \\ Y\xi_0 \end{bmatrix} \tag{105}$$

as the $m+n+1 = 5+1$-dimensional augmented state vector, Eqs. (102)-(104) can be combined to a single differential equations system:

$$\dot{\mathbf{Z}} = \mathbf{C}\mathbf{Z} \tag{106}$$

with

$$\mathbf{C} := \begin{bmatrix} \mathbf{0}_{m\times m} & \mathbf{0}_{m\times n} & \frac{k_e}{\xi_0}\mathbf{P}^e\dot{\mathbf{e}} \\ \mathbf{0}_{n\times m} & \mathbf{0}_{n\times n} & \frac{1}{(Z^0)^\beta\xi_0^{(1-\beta)}}\mathbf{P}^s\dot{\mathbf{s}} \\ \frac{k_e(k_e+k_b)}{H_m}(\mathbf{P}^e\dot{\mathbf{e}})^{\mathrm{T}} & \frac{(k_e+k_b)(Z^0)^\beta}{H_m\xi_0^\beta}(\mathbf{P}^s\dot{\mathbf{s}})^{\mathrm{T}} & 0 \end{bmatrix}, \tag{107}$$

where H_m defined by Eq. (48) can be written as

$$H_m = \frac{k_e\xi_0}{(Z^0)^2}\|\mathbf{Z}^{s(m)}\|^2 + k_b\xi_0. \tag{108}$$

Now we turn our attention to reveal the underlying space of the above system. The yield condition as expressed by Eq. (56) can be written as, after multiplying both sides by Y^2,

$$\|Y\mathbf{P}^e\boldsymbol{\xi}\|^2 + \|Y\mathbf{P}^s\boldsymbol{\xi}\|^2 = (Y\xi_0)^2. \tag{109}$$

In terms of $\mathbf{Z}^{s(m)}$, $\mathbf{Z}^{s(n)}$ and Z^0 the above equation further changes to

$$\|\mathbf{Z}^{s(m)}\|^2 + \left(\frac{Z^0}{\xi_0}\right)^{2\beta}\|\mathbf{Z}^{s(n)}\|^2 = (Z^0)^2. \tag{110}$$

If we introduce the following metric:

$$\boldsymbol{\eta} := \begin{bmatrix} \mathbf{I}_m & \mathbf{0}_{m\times n} & \mathbf{0}_{m\times 1} \\ \mathbf{0}_{n\times m} & \left(\frac{Z^0}{\xi_0}\right)^{2\beta}\mathbf{I}_n & \mathbf{0}_{n\times 1} \\ \mathbf{0}_{1\times m} & \mathbf{0}_{1\times n} & -1 \end{bmatrix}, \tag{111}$$

then by Eqs. (110) and (105) we eventually arrive at

$$\mathbf{Z}^{\mathrm{T}}\boldsymbol{\eta}\mathbf{Z} = 0. \tag{112}$$

The space of $\mathbf{Z}$ endowed with the above metric $\boldsymbol{\eta}$, which depends on the temporal component Z^0, is known as a pseudo-Riemann manifold, which is locally a pseudo-Euclidean space denoted by $\mathbb{E}^6_{5,1}$; and the above equation signifies a distorted cone in a non-flat Minkowski space (Liu, 2003, 2004d).

6.2 A consistent numerical scheme

The evolution of $\mathbf{Z}$ is governed by Eq. (106) with its state matrix $\mathbf{C}$ given by Eq. (107). Due to the piecewise linearity of controlled strain and controlled stress, $\mathbf{P}^e\dot{\mathbf{e}}$ and $\mathbf{P}^s\dot{\mathbf{s}}$ are constant at each time step. Unluckily, due to the presence of Z^0 and $\|\mathbf{Z}^{s(m)}\|^2$ in Eq. (107), this is not true for matrix $\mathbf{C}$. Therefore we approximate the solution of Eq. (106) by considering Z^0 and $\|\mathbf{Z}^{s(m)}\|$ constant in each time step. Under these additional hypotheses, the matrix $\mathbf{C}$ is constant, and so the solution of Eq. (106) is found to be

$$\mathbf{Z}(\ell+1) = \mathbf{G}_z(\ell)\mathbf{Z}(\ell), \tag{113}$$

where

$$\mathbf{G}_z(\ell) := \exp[\Delta t\mathbf{C}(\ell)] = \begin{bmatrix} \mathbf{I}_5 + \frac{[a_z(\ell)-1]}{\mathbf{U}(\ell)\cdot\mathbf{V}(\ell)}\mathbf{U}(\ell)\mathbf{V}^{\mathrm{T}}(\ell) & \frac{b_z(\ell)\mathbf{U}(\ell)}{\sqrt{\mathbf{U}(\ell)\cdot\mathbf{V}(\ell)}} \\ \frac{b_z(\ell)\mathbf{V}^{\mathrm{T}}(\ell)}{\sqrt{\mathbf{U}(\ell)\cdot\mathbf{V}(\ell)}} & a_z(\ell) \end{bmatrix}, \tag{114}$$

in which

$$\mathbf{U} := \begin{bmatrix} \frac{k_e}{\xi_0}\mathbf{P}^e\dot{\mathbf{e}} \\ \frac{1}{(Z^0)^\beta \xi_0^{(1-\beta)}}\mathbf{P}^s\dot{\mathbf{s}} \end{bmatrix}, \tag{115}$$

$$\mathbf{V} := \begin{bmatrix} \frac{k_e(k_e+k_b)}{H_m}\mathbf{P}^e\dot{\mathbf{e}} \\ \frac{(k_e+k_b)(Z^0)^\beta}{H_m\xi_0^\beta}\mathbf{P}^s\dot{\mathbf{s}} \end{bmatrix}, \tag{116}$$

and

$$a_z(\ell) := \cosh(\Delta t\sqrt{\mathbf{U}(\ell)\cdot\mathbf{V}(\ell)}), \tag{117}$$

$$b_z(\ell) := \sinh(\Delta t\sqrt{\mathbf{U}(\ell)\cdot\mathbf{V}(\ell)}). \tag{118}$$

Once $\mathbf{Z}^{s(m)}(\ell+1)$, $\mathbf{Z}^{s(n)}(\ell+1)$ and $Z^0(\ell+1)$ are calculated from Eq. (113), $Y(\ell+1)$, $\mathbf{P}^e\boldsymbol{\xi}(\ell+1)$ and $\mathbf{P}^s\boldsymbol{\xi}(\ell+1)$ can be calculated by

$$Y(\ell+1) = \frac{Z^0(\ell+1)}{\xi_0}, \tag{119}$$

$$\mathbf{P}^e\boldsymbol{\xi}(\ell+1) = \frac{\mathbf{Z}^{s(m)}(\ell+1)}{Y(\ell+1)}, \tag{120}$$

$$\mathbf{P}^s\boldsymbol{\xi}(\ell+1) = \frac{\mathbf{Z}^{s(n)}(\ell+1)}{Y^{(1-\beta)}(\ell+1)}. \tag{121}$$

Substituting the latter two equations into Eqs. (51)-(54) we obtain $\mathbf{P}^e\mathbf{s}(\ell+1)$, $\mathbf{P}^s\mathbf{e}(\ell+1)$, $\boldsymbol{\alpha}(\ell+1)$ and $\mathbf{e}^p(\ell+1)$. From Eqs. (113), (114) and (105) we obtain

$$\begin{bmatrix} Y(\ell+1)\mathbf{P}^e\boldsymbol{\xi}(\ell+1) \\ y(\ell+1)\mathbf{P}^s\boldsymbol{\xi}(\ell+1) \end{bmatrix} = \begin{bmatrix} Y(\ell)\mathbf{P}^e\boldsymbol{\xi}(\ell) \\ y(\ell)\mathbf{P}^s\boldsymbol{\xi}(\ell) \end{bmatrix} + \left(\frac{[a_z(\ell)-1]c(\ell)Y(\ell)}{\mathbf{U}(\ell)\cdot\mathbf{V}(\ell)} + \frac{\xi_0 b_z(\ell)Y(\ell)}{\sqrt{\mathbf{U}(\ell)\cdot\mathbf{V}(\ell)}}\right)\mathbf{U}(\ell), \tag{122}$$

$$Y(\ell+1)\xi_0 = \frac{b_z(\ell)c(\ell)Y(\ell)}{\sqrt{\mathbf{U}(\ell)\cdot\mathbf{V}(\ell)}} + \xi_0 a_z(\ell)Y(\ell), \tag{123}$$

where

$$c(\ell) = \frac{k_e+k_b}{H_m(\ell)}\boldsymbol{\xi}(\ell)\cdot\dot{\mathbf{u}}(\ell). \tag{124}$$

Eq. (122) dividing by Eq. (123) and deleting $Y(\ell)$ in both the numerator and denominator we get two equations:

$$\mathbf{P}^e\boldsymbol{\xi}(\ell+1) = \xi_0\mathbf{W}_1(\ell), \tag{125}$$

$$\mathbf{P}^s\boldsymbol{\xi}(\ell+1) = \frac{\xi_0}{Y^{-\beta}(\ell+1)}\mathbf{W}_2(\ell), \tag{126}$$

where

$$d(\ell) := \frac{k_e+k_b}{\xi_0 H_m(\ell)}\|\dot{\mathbf{u}}(\ell)\|^2, \tag{127}$$

$$\mathbf{W}_1(\ell) = \frac{\mathbf{P}^e\boldsymbol{\xi}(\ell) + \left[\frac{k_e[a_z(\ell)-1]c(\ell)}{\xi_0 d(\ell)} + \frac{k_e b_z(\ell)}{\sqrt{d(\ell)}}\right]\mathbf{P}^e\dot{\mathbf{e}}(\ell)}{a_z(\ell)\xi_0 + \frac{b_z(\ell)c(\ell)}{\sqrt{d(\ell)}}}, \tag{128}$$

$$\mathbf{W}_2(\ell) = Y^{-\beta}(\ell)\frac{\mathbf{P}^s\boldsymbol{\xi}(\ell) + \left[\frac{[a_z(\ell)-1]c(\ell)}{\xi_0 d(\ell)} + \frac{b_z(\ell)}{\sqrt{d(\ell)}}\right]\mathbf{P}^s\dot{\mathbf{s}}(\ell)}{a_z(\ell)\xi_0 + \frac{b_z(\ell)c(\ell)}{\sqrt{d(\ell)}}} \tag{129}$$

are all known from the previous time step.

Substituting Eqs. (125) and (126) into the yield condition (56), and solve it for $Y^{-\beta}(\ell+1)$ we obtain

$$Y^{-\beta}(\ell+1) = \sqrt{\frac{\|\mathbf{W}_2(\ell)\|^2}{1-\|\mathbf{W}_1(\ell)\|^2}}. \tag{130}$$

Once $Y^{-\beta}$ is substituted into Eqs. (125) and (126), it is easy to check that

$$\|\mathbf{P}^e\boldsymbol{\xi}(\ell+1)\|^2 + \|\mathbf{P}^s\boldsymbol{\xi}(\ell+1)\|^2 = \xi_0^2, \tag{131}$$

and thus we get a consistent numerical scheme without needing for any iterations.

7 Radial-return method

In this section we briefly discuss the radial return method for the mixed-control case. This method requires two steps to search a suitable increment of $\Delta\lambda(\ell+1)$: the first step is to find the trial stress state with an elastic prediction, and then the second step is to correct the stress to satisfy the consistency condition.

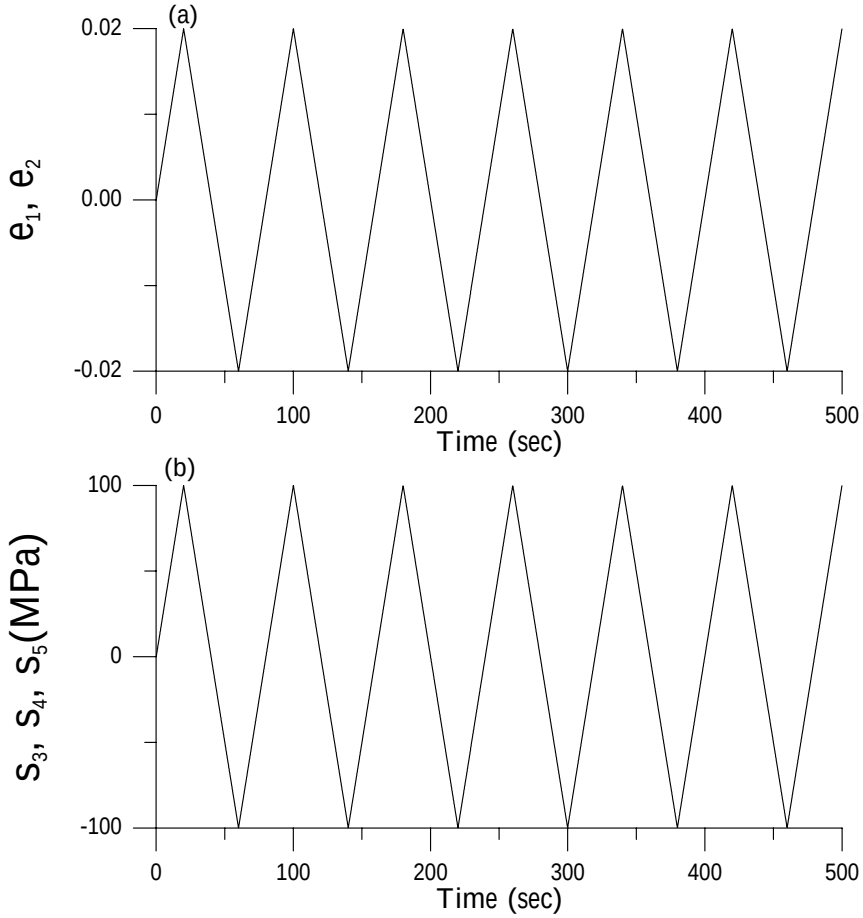

Figure 2 : The time histories of strain and stress mixed-control.

The updated active stress is determined by Eq. (46) with an incremental form:

$$\boldsymbol{\xi}(\ell+1) = \boldsymbol{\xi}(\ell) + k_e \mathbf{P}^e \Delta\mathbf{e} + \mathbf{P}^s \Delta\mathbf{s} - \frac{(k_e+k_b)\Delta\lambda(\ell+1)}{\xi_0}\mathbf{P}^e\boldsymbol{\xi}(\ell) - \frac{k_b\Delta\lambda(\ell+1)}{\xi_0}\mathbf{P}^s\boldsymbol{\xi}(\ell). \tag{132}$$

From the above equation we can calculate $\boldsymbol{\xi}(\ell+1)$ if $\Delta\lambda(\ell+1)$ is calculated.

In order to get $\Delta\lambda(\ell+1)$, let us insert the above equation into the consistency condition $\|\boldsymbol{\xi}(\ell+1)\| = \xi_0^2$:

$$A[\Delta\lambda(\ell+1)]^2 + B\Delta\lambda(\ell+1) + C = 0, \tag{133}$$

where

$$A := \frac{(k_e+k_b)^2}{\xi_0^2}\|\mathbf{P}^e\boldsymbol{\xi}(\ell)\|^2 + \frac{k_b^2}{\xi_0^2}\|\mathbf{P}^s\boldsymbol{\xi}(\ell)\|^2, \tag{134}$$

$$B := \frac{-2(k_e+k_b)}{\xi_0}\boldsymbol{\xi}(\ell)\cdot\mathbf{P}^e\boldsymbol{\xi}(\ell) - \frac{2k_b}{\xi_0}\boldsymbol{\xi}(\ell)\cdot\mathbf{P}^s\boldsymbol{\xi}(\ell) - \frac{2k_e(k_e+k_b)}{\xi_0}\Delta\mathbf{e}\cdot\mathbf{P}^e\boldsymbol{\xi}(\ell) - \frac{2k_b}{\xi_0}\Delta\mathbf{s}\cdot\mathbf{P}^s\boldsymbol{\xi}(\ell), \tag{135}$$

$$C := \|k_e\mathbf{P}^e\Delta\mathbf{e}\|^2 + \|\mathbf{P}^s\Delta\mathbf{s}\|^2 + 2k_e\boldsymbol{\xi}(\ell)\cdot\mathbf{P}^e\Delta\mathbf{e} + 2\boldsymbol{\xi}(\ell)\cdot\mathbf{P}^s\Delta\mathbf{s} + \|\boldsymbol{\xi}(\ell)\|^2 - \xi_0^2. \tag{136}$$

Because Eq. (133) is a quadratic equation we can solve it to obtain

$$\Delta\lambda(\ell+1) = \frac{-B-\sqrt{B^2-4AC}}{2A}. \tag{137}$$

Inserting the above $\Delta\lambda(\ell+1)$ into Eq. (132) the updated active stress can be determined. Then from Eqs. (51) and (52) we obtain $\mathbf{P}^e\mathbf{s}$ and $\mathbf{P}^s\mathbf{e}$, respectively. Inserting these vectors into Eqs. (53) and (54) we thus obtain $\boldsymbol{\alpha}$ and $\mathbf{e}^p$, respectively.

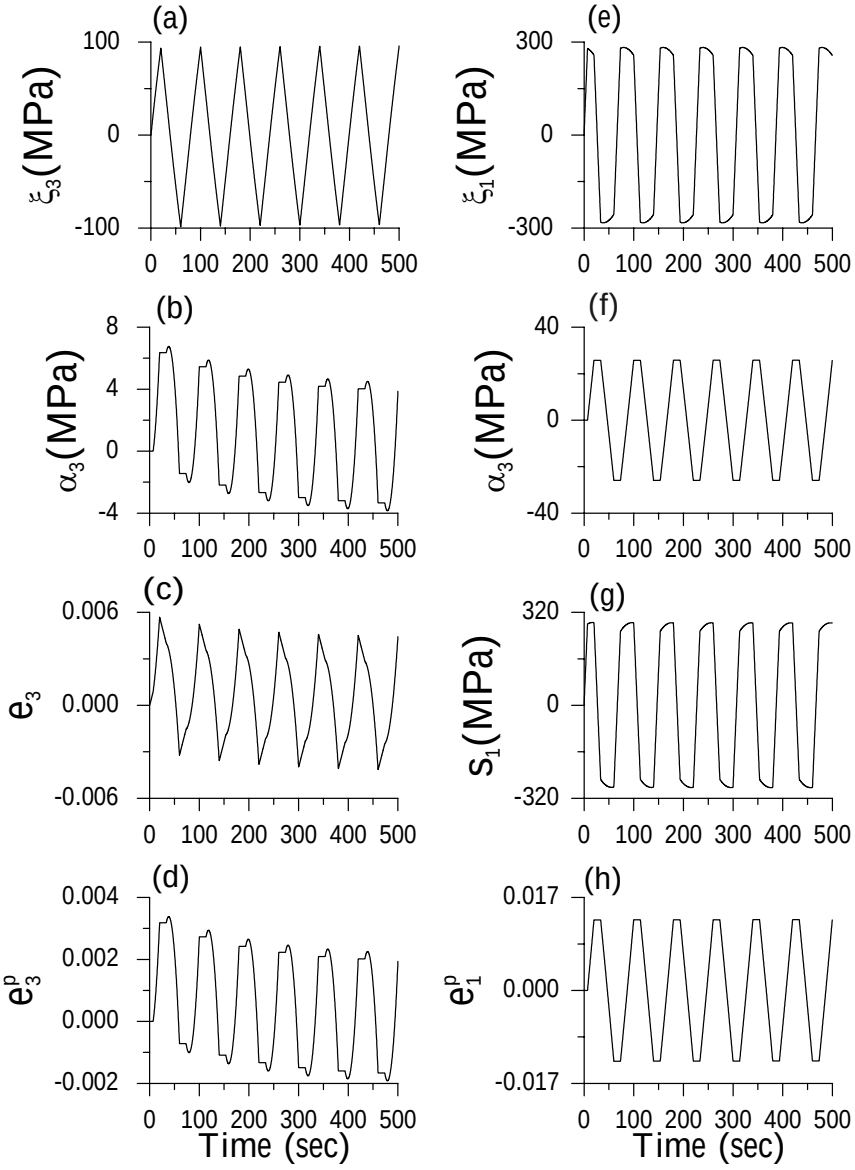

Figure 3 : The time histories of responses under a mixed-control.

8 Numerical examples

In the above three sections we have derived three schemes, namely, group preserving scheme (GPS), pseudo-Riemann method (PRM) and radial return method (RRM). In this section numerical examples are used to test these three numerical schemes.

In order to assess the performances of the above three numerical methods we employ a numerical example with $\mathbf{P}^e = \text{diag}\,[1,1,0,0,0]$, which means that the strain control components are e_1 and e_2 and the stress control components are s_3, s_4 and s_5. In Fig. 2 the time histories of the mixed-controlled components are plotted. In all numerical calculations the material constants are fixed to be $k_e = 40000$ MPa, $\xi_0 = 400$ MPa, and $k_b = 2000$ MPa. The time step size used is $\Delta t = 0.01$ sec.

Since the first mixed-control path used to testing is a piecewise linear one, of which $\mathbf{P}^e\dot{\mathbf{e}}$ and $\mathbf{P}^s\dot{\mathbf{s}}$ are constant, we can calculate the responses in the elastic phase by

$$\mathbf{P}^e\mathbf{s}(t) = \mathbf{P}^e\mathbf{s}(t_i) + k_e(t-t_i)\mathbf{P}^e\dot{\mathbf{e}}, \tag{138}$$

$$\mathbf{P}^e\boldsymbol{\xi}(t) = \mathbf{P}^e\boldsymbol{\xi}(t_i) + k_e(t-t_i)\mathbf{P}^e\dot{\mathbf{e}}, \tag{139}$$

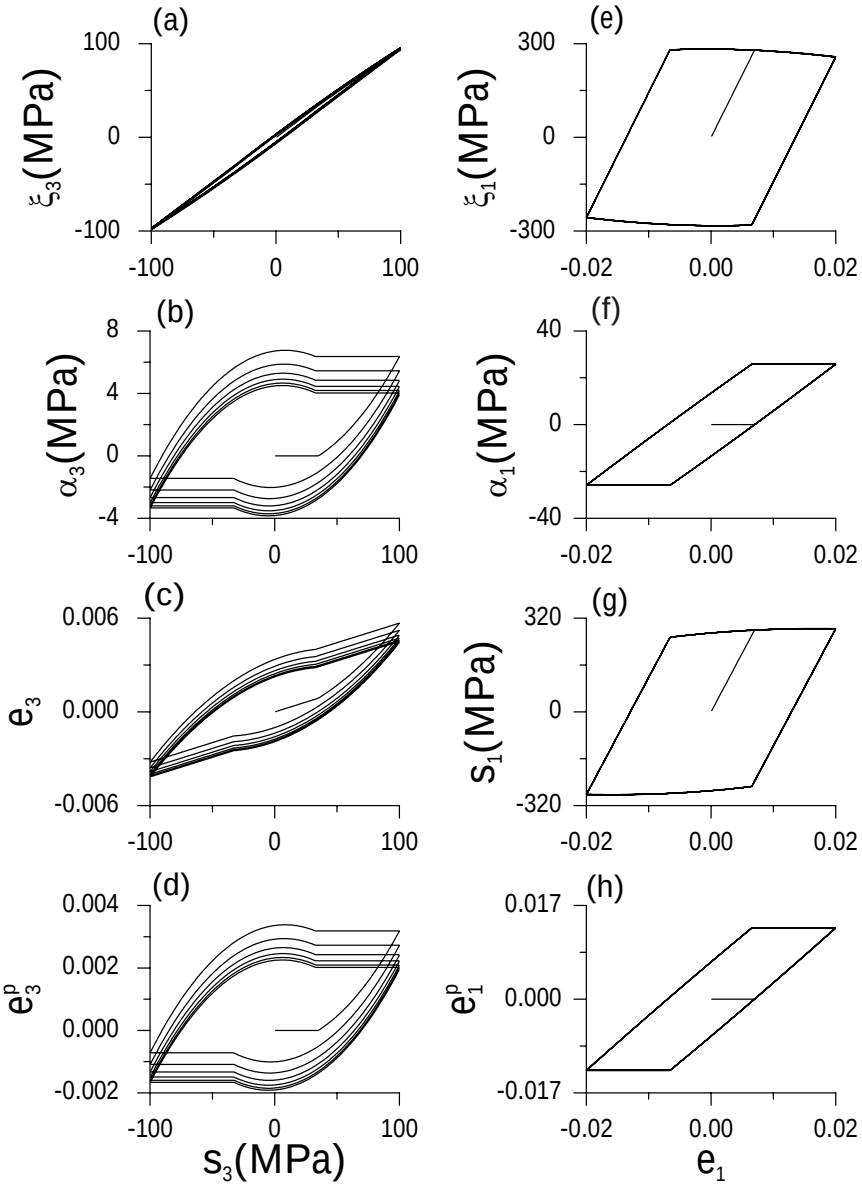

Figure 4 : The hysteretic loops of responses under a mixed-control.

$$\mathbf{P}^s\mathbf{e}(t) = \mathbf{P}^s\mathbf{e}(t_i) + \frac{1}{k_e}(t-t_i)\mathbf{P}^s\dot{\mathbf{s}}, \tag{140}$$

$$\mathbf{P}^s\boldsymbol{\xi}(t) = \mathbf{P}^s\boldsymbol{\xi}(t_i) + (t-t_i)\mathbf{P}^s\dot{\mathbf{s}}. \tag{141}$$

The end time of an elastic phase is determined by solving the following equation, obtained by substituting Eq. (139) for $\mathbf{P}^e\boldsymbol{\xi}$ and Eq. (141) for $\mathbf{P}^s\boldsymbol{\xi}$ into Eq. (56):

$$A(t-t_i)^2 + B(t-t_i) + C = 0, \tag{142}$$

where

$$A = k_e^2\dot{\mathbf{e}}\cdot\mathbf{P}^e\dot{\mathbf{e}} + \dot{\mathbf{s}}\cdot\mathbf{P}^s\dot{\mathbf{s}}, \tag{143}$$

$$B = 2k_e\mathbf{P}^e\boldsymbol{\xi}(t_i)\cdot\mathbf{P}^e\dot{\mathbf{e}} + 2\mathbf{P}^s\boldsymbol{\xi}(t_i)\cdot\mathbf{P}^s\dot{\mathbf{s}}, \tag{144}$$

$$C = \boldsymbol{\xi}(t_i)\cdot\mathbf{P}^e\boldsymbol{\xi}(t_i) + \boldsymbol{\xi}(t_i)\cdot\mathbf{P}^s\boldsymbol{\xi}(t_i) - \xi_{s0}^2. \tag{145}$$

We plot the time histories of responses in Fig. 3, including active stress, back stress, stress and plastic strain. The first row is the responses that correspond to the stres control of s_3, while the second row is the responses that correspond to the strain control of e_1. For saving space we do not plot the other components of responses, which are similar to the above ones. In addition we also plot the

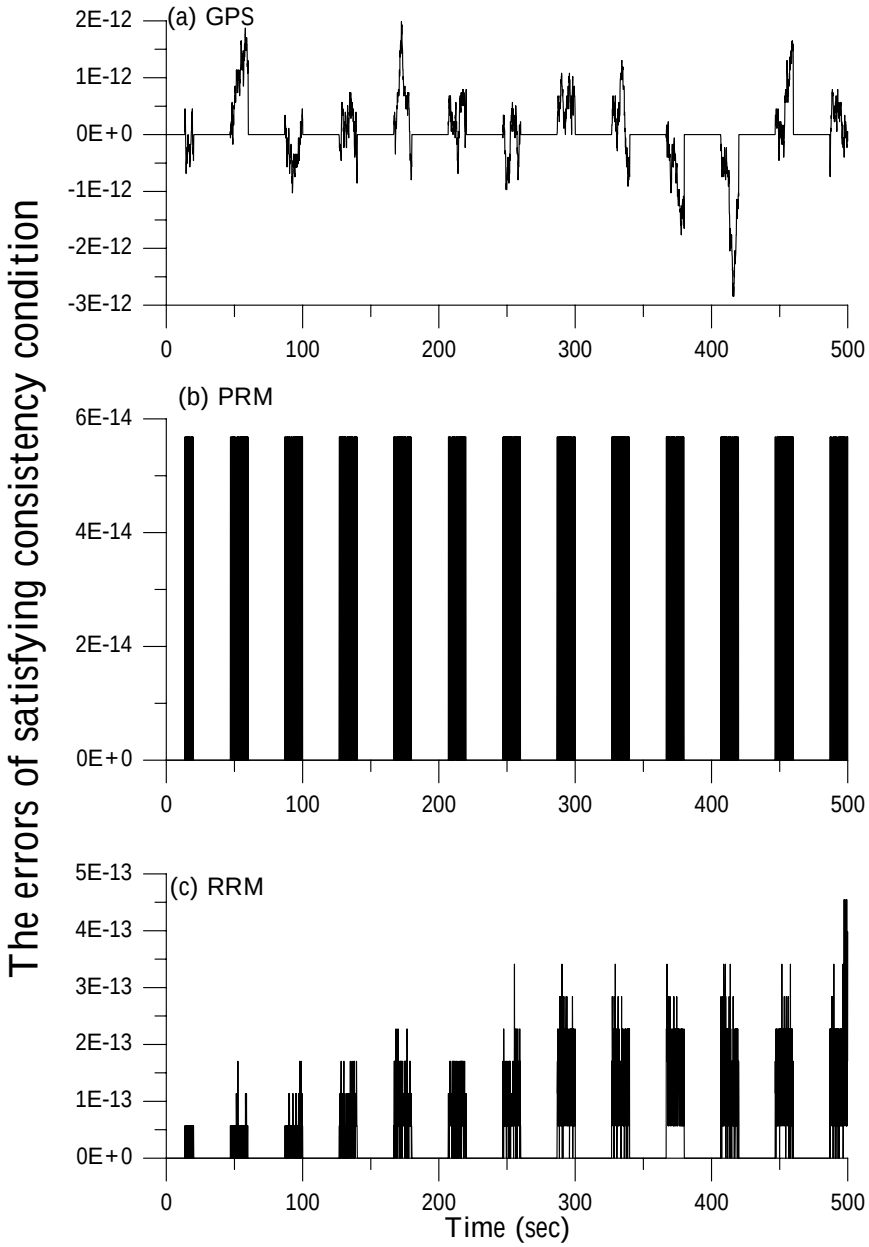

Figure 5 : Comparing the errors by satisfying the consistency condition of (a) GPS, (b) PRM and (c) RRM.

control-based responses in Fig. 4, where different types of hysteresis loops can be seen. The left-hand figures display prominent relaxations of responses under cyclic stress control.

In Fig. 5 we display the errors of satisfying the consistency condition. It can be seen that PRM gives almost zero value of the error of the consistency condition defined by $\mathbf{ERR}_1 := \|\boldsymbol{\xi}\| - s_0$, while RRM has the error of the consistency condition within the order of 5×10^{-13}. Because GPS needs a numerical solution to obtain $\xi_e(\ell+1)$ by Eq. (99), the consistency error of GPS is slightly larger than that of RRM and PRM within the order of 3×10^{-12}. Needless to say PRM is the best one of these three numerical methods to satisfy the consistency condition.

In order to give a more refined criterion to assess the performance, let us introduce the following strain and stress relative errors at a given discrete time $t(m)$ for the above

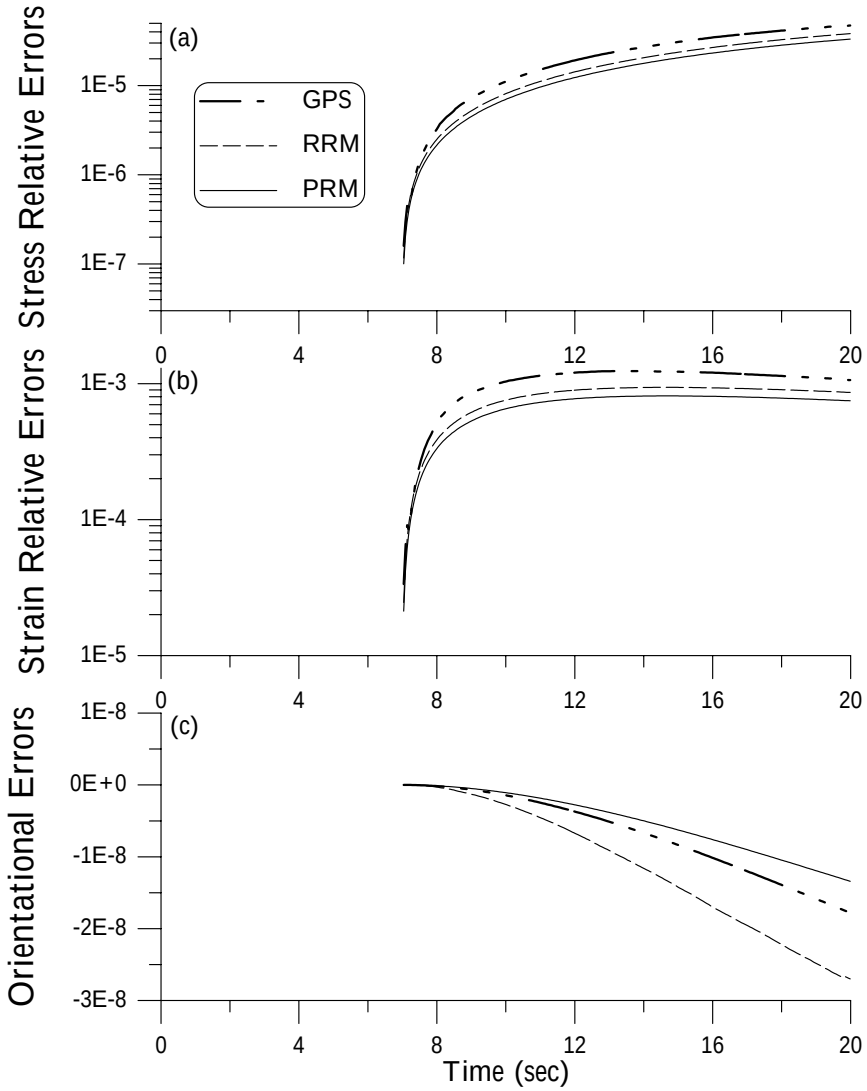

Figure 6 : Comparing (a) stress relative errors, (b) strain relative errors and (c) orientational errors for GPS, RRM and PRM.

mixed loading case:

$$\mathbf{ERR}_2 := \frac{\|\mathbf{s}(m) - \mathbf{s}^*(m)\|}{\sup_{j\in\{0,1,\ldots,m\}}\|\mathbf{s}^*(m)\|}, \tag{146}$$

$$\mathbf{ERR}_3 := \frac{\|\mathbf{e}(m) - \mathbf{e}^*(m)\|}{\sup_{j\in\{0,1,\ldots,m\}}\|\mathbf{e}^*(m)\|}, \tag{147}$$

where $\mathbf{e}^*(m)$, $\mathbf{e}(m)$, $\mathbf{s}^*(m)$ and $\mathbf{s}(m)$ are strain and stress vectors, containing respectively the "exact" and the numerical solutions at time $t(m)$. For the mixed-control case it must consider both the effects of each strain and stress control at the same time. For the considered model, because of the lack of closed-form solution of the problem under investigation, we computed the numerical solution with a finer time interval $\Delta t = 0.005$ sec; the differences between such "exact" solution with other numerical solutions with more practical and larger time steps were then used to assess the performance of numerical schemes. In Figs. 6(a) and 6(b) we show the stress and strain relative errors for GPS, RRM and PRM in the plastic state by using a time step size with $\Delta t = 0.01$ sec. The good results obtained with PRM can be immediately appreciated.

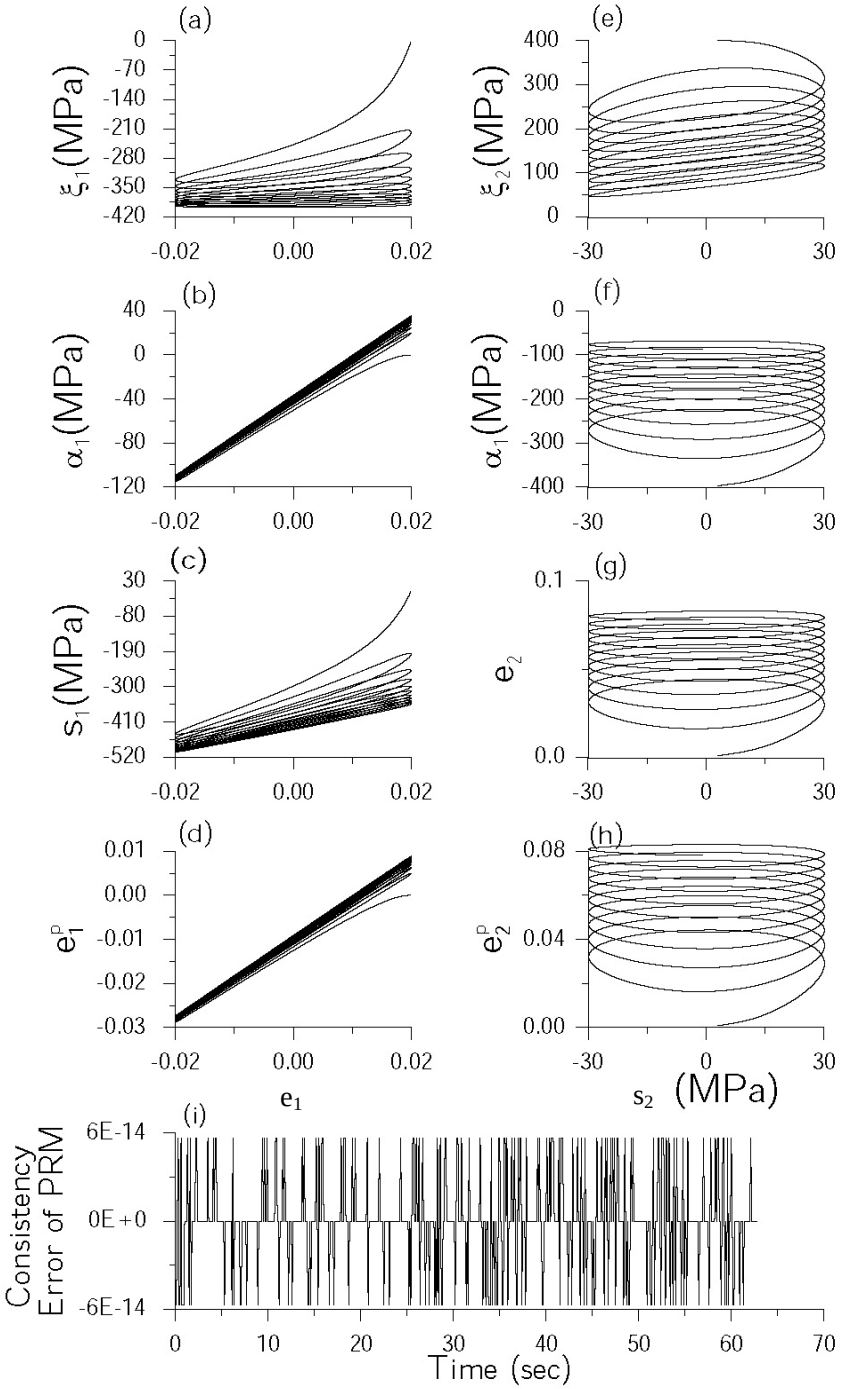

Figure 7 : The cyclic responses under a non-proportional circular mixed-control path are plotted in (a)-(h). The consistency error induced by PRM is plotted in (i).

Let us further consider an orientational error defined by

$$\mathbf{ERR}_4 := \frac{\boldsymbol{\xi}(m)\cdot\boldsymbol{\xi}^*(m)}{\xi_0^2} - 1. \tag{148}$$

Fig. 6(c) shows the orientational errors for GPS, RRM and PRM. It can be seen that the errors of PRM and GPS are far less than that of RRM.

Next, we consider a non-proportional loading case with

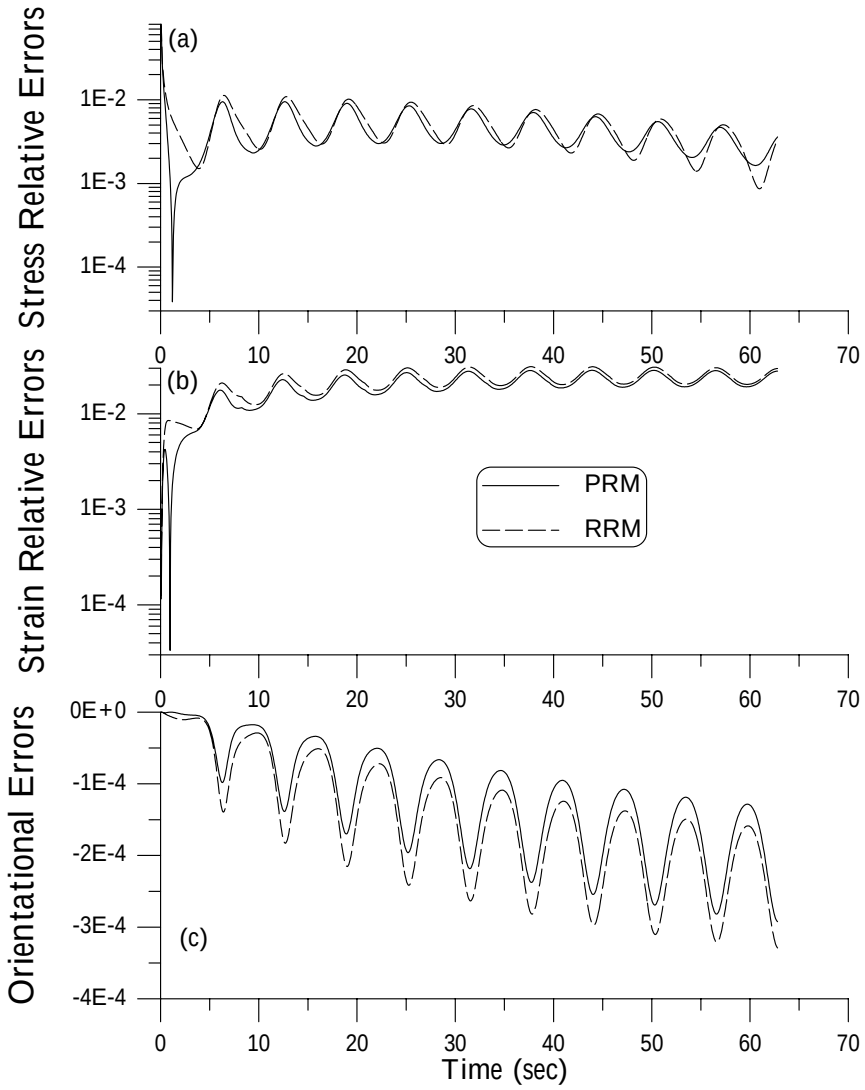

Figure 8 : Comparing (a) stress relative errors, (b) strain relative errors and (c) orientational errors for RRM and PRM.

the input a two-dimensional circular path:

$$e_1(t) = e_0 \cos t, \;\; s_2(t) = s_0 \sin t. \tag{149}$$

In order to investigate the consistency conditions of these numerical schemes, we let $s_1 = 0$ MPa and $s_2 = 400$ MPa be located on the yield surface initially and let $e_0 = 0.02$ and $s_0 = 30$ MPa be large enough such that under the above cyclic loading the material is always in the plastic state. The material constants used are the same as that in the above but with $k_b = 4000$ MPa. In Figs. 7(a)-7(h) we plot the cyclic responses under ten cycles of the above loading. The consistency error induced by the numerical scheme of PRM is plotted in Fig. 7(i). As expected this numerical scheme preserves the consistency condition very well; however, the nonzero values presented in the figure are due to the machinery round off errors. In Fig. 8 we compare the stress and strain relative errors and the orientational errors of RRM and PRM.

9 Conclusions

Three consistency-preserving integrators of a plasticity model with Prager's kinematic hardening rule under strain and stress mixed-controls were developed. The group preserving algorithm results from our investigation of the plasticity equations by a Lie group symmetry study of the augmented quasi-linear differential equations systems and a twin-cone structure in the product space of

$\mathbb{M}^{m+1} \otimes \mathbb{M}^{n+1}$, where m and n are respectively the numbers of strain and stress control components.

Even though the constitutive equations are highly nonlinear under mixed-controls, through an integrating factor and a single cone structure they can be converted to a Lie type system $\dot{\mathbf{Z}} = \mathbf{CZ}$ in the $5+1$-dimensional augmented stress space of $\mathbf{Z}$. In the augmented stress space an internal spacetime structure of the pseudo-Riemannian type is brought out. The control tensor $\mathbf{C}$ for the plastic phase was proved to be an element of the real Lie algebra $sl(5,1,\mathbb{R})$ of the special orthochronous pseudo-linear group $SL(5,1,\mathbb{R})$. In addition the material hardening and anisotropy, which cause the internal spacetime non-flat, this study has also shown that the mechanism of mixed-control may cause the non-flatness of internal spacetime.

According to these symmetry studies, numerical schemes which preserve the group properties for every time increment were developed. These group preserving schemes may be specifically called consistent schemes, since they are capable of updating the stress point to be located on the yield surface at the end of each time increment in the plastic phase. Especially, the PRM algorithm is the best one, which updates stress point on the yield surface without needing for any iterations.

Numerical examples were used to assess the performance of the new algorithms. In terms of the errors by satisfying the consistency condition, strain and stress relative errors and the orientational errors, we have shown that the new algorithm of PRM provided good accuracy.

Acknowledgement: The financial support provided by the National Science Council of Taiwan under the Grant NSC 92-2212-E-019-006 is gratefully acknowledged.

References

Hong, H.-K.; Liu, C.-S. (1999a): Internal symmetry in bilinear elastoplasticity. *Int. J. Non-Linear Mech.*, vol. 34, pp. 279-288.

Hong, H.-K.; Liu, C.-S. (1999b): Lorentz group $SO_o(5,1)$ for perfect elastoplasticity with large deformation and a consistency numerical scheme. *Int. J. Non-Linear Mech.*, vol. 34, pp. 1113-1130.

Hong, H.-K.; Liu, C.-S. (2000): Internal symmetry in the constitutive model of perfect elastoplasticity. *Int. J. Non-Linear Mech.*, vol. 35, pp. 447-466.

Hong, H.-K.; Liu, C.-S. (2001): Some physical models with Minkowski spacetime structure and Lorentz group symmetry. *Int. J. Non-Linear Mech.*, vol. 36, pp. 1075-1084.

Klisinski, M. (1998): On constitutive relations for arbitrary stress-strain control in multi-surface plasticity. *Int. J. Solids Struct.*, vol. 35, pp. 2655-2678.

Klisinski, M.; Mróz, Z.; Runesson, K. (1992): Structure of constitutive equations in plasticity for different choices of state and control variables. *Int. J. Plasticity*, vol. 8, pp. 221-243.

Lang, S. (1999): Fundamentals of Differential Geometry. Springer-Verlag, New York.

Liu, C.-S. (2001): Cone of non-linear dynamical system and group preserving schemes. *Int. J. Non-Linear Mech.*, vol. 36, pp. 1047-1068.

Liu, C.-S. (2002): The steady-state responses of a bilinear elastoplastic oscillator under sinusoidal loading. *J. Chinese Inst. Engr.*, vol. 25, pp. 199-210.

Liu, C.-S. (2003): Symmetry groups and the pseudo-Riemann spacetimes for mixed-hardening Elastoplasticity. *Int. J. Solids Struct.*, vol. 40, pp. 251-269.

Liu, C.-S. (2004a): A consistent numerical scheme for the von Mises mixed-hardening constitutive equations. *Int. J. Plasticity*, vol. 20, pp. 663-704.

Liu, C.-S. (2004b): Lie symmetries of finite strain elastic-perfectly plastic models and exactly consistent schemes for numerical integrations. *Int. J. Solids Struct.*, vol. 41, pp. 1823-1853.

Liu, C.-S. (2004c): Internal symmetry groups for the Drucker-Prager material model of plasticity and numerical integrating methods. *Int. J. Solids Struct.*, vol. 41, pp. 3771-3791.

Liu, C.-S. (2004d): Internal symmetry groups for perfect elastoplasticity under axial-torsional loadings. *J. Chinese Inst. Engr.*, vol. 27, pp. 993-1002.

Liu, C.-S. (2005): Computational applications of the Poincaré group on the elastoplasticity with kinematic hardening. *CMES: Computer Modeling in Engineering & Sciences*, vol. 8, pp. 231-258.

Liu, C.-S.; Chang, C.-W. (2004): Lie group symmetry applied to the computation of convex plasticity constitutive equation. *CMES: Computer Modeling in Engineering & Sciences*, vol. 6, 277-294.

Liu, C.-S.; Chang, C.-W. (2005): Non-canonical Minkowski and pseudo-Riemann frames of plasticity

models with anisotropic quadratic yield criteria. *Int. J. Solids Struct.*, vol. 42, pp. 2851-2882.

Liu, C.-S.; Li, C.-F. (2005): Geometrical numerical algorithms for a plasticity model with Armstrong-Frederick kinematic hardening rule under strain and stress controls. *Int. J. Num. Meth. Eng.*, vol. 63, pp. 1396-1423.

Naylor, A. W.; Sell, G. R. (1982): Linear Operator Theory in Engineering and Science. Springer-Verlag, New York.

Prager, W. (1956): A new method of analyzing stresses and strains in work-hardening plastic solids. *J. Appl. Mech. ASME*, vol. 23, pp. 493-496.

Ritto-Corrêa, M.; Camotim, D. (2001): Integration algorithm for J_2 elastoplasticity under arbitrary mixed stress-strain control. *Int. J. Num. Meth. Eng.*, vol. 50, pp. 1213-1232.